Acta Mech 227, 1743–1751 (2016)
DOI 10.1007/s00707-016-1591-8

ORIGINAL PAPER

A. Matta · P. A. L. Narayana · A. A. Hill

Nonlinear thermal instability in a horizontal porous layer with an internal heat source and mass flow

Received: 13 August 2015 / Revised: 12 February 2016 / Published online: 9 March 2016

Abstract Linear and nonlinear stability analyses of Hadley–Prats flow in a horizontal fluid-saturated porous medium with a heat source are performed. The results indicate that, in the linear case, an increase in the horizontal thermal Rayleigh number is stabilizing for both positive and negative values of mass flow. In the nonlinear case, a destabilizing effect is identified at higher mass flow rates. An increase in the heat source has a destabilizing effect. Qualitative changes appear in R_z as the mass flow moves from negative to positive for different internal heat sources.

1 Introduction

Thermal convection driven by an internal heat source with a horizontal mass flow has many practical applications such as underground energy transport, cooling of nuclear reactors, food processing, oil recovery, underground storage of waste products and thermal convection in clouds [1–4].

In the last few decades, convection involving internal heat sources has attracted particular research attention. Early experimental investigations include Schwiderski and Schwabh [5] and Tritton and Zarraua [6], with Roberts [7] and Thirlby [8] providing theoretical analyses. Parthiban and Patil [9] investigated thermal convection due to non-uniform heating boundaries with inclined thermal gradients in the presence of an internal heat source, followed by an extension to anisotropic porous layers by Parthiban and Patil [10]. The case of an inclined layer with internal heat source was analyzed by Barletta et al. [11], where both boundaries were isothermal and kept at the same temperatures. Rionero and Straughan [12] investigated the linear and nonlinear effects in the presence of variable gravity effect and heat generation. Extensive reviews of the theory and applications can be found in the article by Alex and Patil [13]. Hill [14] investigated a porous layer with concentration-based internal heat generation, with linear and nonlinear stability analyses of thermosolutal convection. Chamka et al. [15] analyzed the effect of an internal heat source or sink for hydromagnetic simultaneous heat and mass transfer by utilizing similarity solutions. Thermosolutal convection in a saturated anisotropic porous medium with internal heat generation is reported by Bhadauria [16]. Borujerdi et al. [17] examined the steady-state heat conduction with a uniform heat source where the solid and fluid phases are at different temperatures. Borujerdi et al. [18] study the influence of the Darcy number on the critical Rayleigh number in the onset of convection with uniform internal heating. A collection of comprehensive theories and experiments of thermal convection in porous media (with their practical applications) has been surveyed by Nield and Bejan [19]. Capone and

A. Matta · P. A. L. Narayana
Department of Mathematics, Indian Institute of Technology Hyderabad, Hyderabad, Telangana 502205, India
E-mail: ananth@iitm.ac.in

A. A. Hill (✉)
Department of Biological, Biomedical and Analytical Sciences, University of the West of England, Bristol BS16 1QY, UK
E-mail: antony.hill@uwe.ac.uk

Rionero [20] have studied the nonlinear stability of a convective motion in a horizontal porous layer which is driven by a temperature gradient. Several problems on nonlinear stability analyses using the energy method are discussed by Kaloni and his contributors [21–25]. In the Lyapunov sense, when the disturbance of the basic flow is unstable, linearized theory provides sufficient conditions, whereas nonlinear theory provides sufficient conditions for the disturbance to be asymptotically stable.

The aim of this article is to study the influences of both a heat source and a mass flow. The corresponding eigenvalue problems are solved numerically utilizing the shooting and Runge–Kutta method.

2 Mathematical analysis

An infinite shallow horizontal fluid-saturated porous medium with thickness d is considered. The z' -axis is vertically upwards, and there is a net flow along the direction of the x'-axis with magnitude M'. The vertical temperature difference across the boundaries is $\triangle\theta$. Further imposed is the horizontal temperature gradient vector $(\beta_{\theta_x},\ \beta_{\theta_y})$. The porous layer flow is governed by the Darcy law, where the linear Boussinesq approximation is assumed. Utilizing the equation of the conservation of energy, the governing equations in dimensional form are

$$\nabla'\cdot q' = 0\ , \tag{1}$$

$$\tfrac{\mu}{K} q' + \nabla' P' - \rho_0 \left[1 - \gamma_\theta \left(\theta' - \theta_0\right)\right] g = 0, \tag{2}$$

$$(\rho c)_m \left(\tfrac{\partial \theta'}{\partial t'}\right) + \left(\rho c_p\right)_f q'\cdot \nabla'\theta' = k_m \nabla'^2 \theta' + Q', \tag{3}$$

with the following boundary conditions:

$$w' = 0, \quad \theta' = \theta_0 - \frac{1}{2}\left(\pm\triangle\theta\right) - \beta_{\theta_x} x' - \beta_{\theta_y} y' \quad \text{at} \quad z' = \pm\frac{\mathrm{d}}{2}. \tag{4}$$

Here, the Darcy velocity is defined as $q' = (u', v', w')$, P' is the pressure, θ' is temperature, and Q' is an internal heat source. The subscripts f and m refer to the fluid and the porous medium, respectively. ϕ and K are the porosity and permeability of the porous layer. c, ρ, μ, k_m and γ_θ denote the specific heat, density, viscosity, thermal diffusivity, and thermal expansion coefficient in the porous medium, respectively.

The following dimensionless variables are introduced to non-dimensionalize the governing equations:

$$\begin{gathered}(x, y, z) = \frac{1}{d}\left(x', y', z'\right), \quad t = \frac{\alpha_m t'}{a d^2}, \quad q = \frac{d q'}{\alpha_m}, \quad P = \frac{K\left(P' + \rho_0 g z'\right)}{\mu\alpha_m}, \\ \theta = \frac{R_z\left(\theta' - \theta_0\right)}{\triangle\theta}, \quad M = \frac{d M'}{\alpha_m}, \quad Q = \frac{d^2 Q'}{k_m \triangle\theta}\end{gathered} \tag{5}$$

where

$$\alpha_m = \frac{k_m}{\left(\rho c_p\right)_f}, \quad a = \frac{(\rho c)_m}{\left(\rho c_p\right)_f}, \quad R_z = \frac{\rho_0 g \gamma_\theta K d \triangle\theta}{\mu\alpha_m}. \tag{6}$$

Here, R_z denotes the vertical thermal Rayleigh number. The horizontal thermal Rayleigh numbers are defined as follows:

$$R_x = \frac{\rho_0 g \gamma_\theta K d^2 \beta_{\theta_x}}{\mu\alpha_m}, \quad R_y = \frac{\rho_0 g \gamma_\theta K d^2 \beta_{\theta_y}}{\mu\alpha_m}. \tag{7}$$

The previous scaling for dimensional variables and the horizontal thermal Rayleigh numbers were introduced by Weber [27] and used extensively by Nield [28]. Under these dimensionless variables, the governing Eqs. (1)–(3) are

$$\nabla\cdot q = 0\ , \tag{8}$$

$$q + \nabla P - \theta\mathbf{k} = 0, \tag{9}$$

$$\tfrac{\partial\theta}{\partial t} + q\cdot\nabla\theta = \nabla^2\theta + Q R_z, \tag{10}$$

with the conditions of the plates being

$$w = 0, \quad \theta = -\frac{1}{2}(\pm R_z) - R_x x - R_y y \quad \text{at} \quad z = \pm\frac{1}{2}. \tag{11}$$

From Eqs. (8)–(10), we observe that all of the thermal Rayleigh numbers are involved in boundary conditions (11). The condition on temperature at both bounding planes give a linear variation of temperature. This spatial linear variation of temperature along the horizontal planes bounding a fluid layer is a physically more realistic situation than the strictly uniform heating (Capone and Rionero [20]). However, in the present problem uniform heating can be recovered by setting the horizontal thermal gradients to zero.

3 Steady-state solution

The flow governing Eqs. (8)–(10), subject to (11), have a basic state solution of the form

$$\begin{aligned} &\theta_s = \widetilde{\theta}(z) - R_x x - R_y y, \\ &u_s = u(z), \quad v_s = v(z), \quad w_s = 0, \quad P_s = P(x, y, z), \end{aligned} \tag{12}$$

with

$$\begin{aligned} u_s &= -\frac{\partial P}{\partial x}, \quad v_s = -\frac{\partial P}{\partial y}, \\ 0 &= -\frac{\partial P}{\partial z} + \widetilde{\theta}(z) - R_x x - R_y y, \\ D^2\widetilde{\theta} &= -u_s R_x - v_s R_y - Q R_z. \end{aligned} \tag{13}$$

Here $D = \frac{\mathrm{d}}{\mathrm{d}z}$, and we have a net flow M in the horizontal direction such that $\int_{-1/2}^{1/2} u(z)\mathrm{d}z = M$ and $\int_{-1/2}^{1/2} v(z)\mathrm{d}z = 0$. The solution in the form of flow velocity and temperature in the medium is then given by

$$u_s = R_x z + M, \quad v_s = R_y z, \tag{14}$$

$$\widetilde{\theta} = -R_z z - \frac{\lambda}{24}\left(4z^3 - z\right) - (MR_x + QR_z)\left(\frac{z^2}{2} - \frac{1}{8}\right) \tag{15}$$

where $\lambda = {R_x}^2 + {R_y}^2$.

4 Perturbation equations

We consider the perturbations in the form $q = q_s + \overline{q}$, $\theta = \theta_s + \overline{\theta}$ and $P = P_s + \overline{P}$. By substituting these perturbations in the dimensionless governing Eqs. (8)–(10), we get

$$\nabla\cdot\overline{q} = 0, \tag{16}$$

$$\overline{q} = -\nabla\overline{P} + \overline{\theta}\mathbf{k}, \tag{17}$$

$$\tfrac{\partial\overline{\theta}}{\partial t} + q_s\cdot\nabla\overline{\theta} + \overline{q}\cdot\nabla\theta_s + \overline{q}\cdot\nabla\overline{\theta} = \nabla^2\overline{\theta} \tag{18}$$

where

$$\begin{aligned} \nabla\theta_s &= -\left(R_x, R_y, R_z - \widetilde{A}\right), \\ \widetilde{A} &= \frac{\lambda}{24}\left[1 - 12z^2\right] - (MR_x + QR_z)\,z. \end{aligned}$$

The conditions at the plates are

$$\overline{w} = 0, \quad \overline{\theta} = 0 \quad \text{at} \quad z = \pm\frac{1}{2}. \tag{19}$$

Note that (19) shows that there are no normal velocity and temperature perturbations at the plates.

5 Linear stability analysis

To perform a linear stability analysis, we neglect the nonlinear terms from Eq. (18). The linearized perturbations equations are then

$$\nabla\cdot\overline{q} = 0, \tag{20}$$

$$\overline{q} = -\nabla\overline{P} + \overline{\theta}\mathbf{k}, \tag{21}$$

$$\tfrac{\partial\overline{\theta}}{\partial t} + q_s\cdot\nabla\overline{\theta} + \overline{q}\cdot\nabla\theta_s = \nabla^2\overline{\theta} \tag{22}$$

where

$$\nabla\theta_s = -\left(R_x,\, R_y,\, R_z - \frac{\lambda}{24}\left[1-12z^2\right] + (MR_x + QR_z)\, z\right).$$

The conditions at the plates are

$$\overline{w} = 0, \quad \overline{\theta} = 0 \quad \text{at} \quad z = \pm\frac{1}{2}\,. \tag{23}$$

Adopting a normal mode solution to Eqs. (20)–(22) of the form

$$\left[\overline{q}, \overline{\theta}, \overline{P}\right] = \left[q\,(z)\,, \theta\,(z)\,, P\,(z)\right]\exp\left\{i\,(kx+ly) + \sigma t\right\} \tag{24}$$

and further eliminating P yields

$$\left(D^2-\alpha^2\right)w + \alpha^2\theta = 0, \tag{25}$$

$$\left(D^2-\alpha^2-(\sigma+i(ku_s+lv_s))\right)\theta + \tfrac{i}{\alpha^2}\left(kR_x+lR_y\right)Dw - \left(D\widetilde{\theta}\right)w = 0. \tag{26}$$

Equations (25) and (26), subject to $w=\theta=0$ at both the plates $z=\frac{1}{2}$ and $z=-\frac{1}{2}$, constitute an eigenvalue problem for the vertical thermal Rayleigh number R_z with a, R_x, R_y, k and l as parameters. In the above, $\alpha=\sqrt{k^2+l^2}$ is the overall wave number. Numerical results are presented in Sect. 7.

6 Nonlinear stability analysis

In this section, our nonlinear analysis via energy functional is presented as follows. We multiply Eqs. (17) and (18) by $\overline{q}$ and $\overline{\theta}$, respectively, and integrate over Ω, where Ω denotes a typical periodicity cell. This yields the following identities:

$$||\overline{q}||^2 = \langle\overline{\theta}\overline{w}\rangle, \tag{27}$$

$$\frac{1}{2}\frac{d||\overline{\theta}||^2}{\mathrm{d}t} = -\langle(\overline{q}\cdot\nabla\theta_s)\,\overline{\theta}\rangle - ||\nabla\overline{\theta}||^2. \tag{28}$$

Here $||\cdot||$ and $\langle\cdot\rangle$ denote the norm and inner product on $L^2(\Omega)$. We adopt the energy functional (cf. [29])

$$E\,(t) = \frac{\xi}{2}\,\|\,\overline{\theta}\,\|^2 \tag{29}$$

with coupling parameter $\xi > 0$. The system of Eqs. (27) and (28) along with Eq. (29) can now be represented in the form

$$\frac{\mathrm{d}E}{\mathrm{d}t} = I - \Delta \tag{30}$$

where

$$I = -\xi\langle(\overline{q}\cdot\nabla\theta_s)\,\overline{\theta}\rangle + \langle\overline{\theta}\overline{w}\rangle, \tag{31}$$

$$\Delta = \xi||\nabla\overline{\theta}||^2 + ||\overline{q}||^2. \tag{32}$$

We define

$$n = \max_{H} \frac{I}{\Delta} \tag{33}$$

where H is the space of all admissible solutions to Eqs. (16)–(18). If $0 < n < 1$, it follows that

$$\frac{\mathrm{d}E}{\mathrm{d}t} \leq -\Delta\,(1-n)\,. \tag{34}$$

The classical Poincare inequality $||\overline{q} - \overline{q}_{\Omega}||_{L^p(\Omega)} \leq C||\nabla\overline{q}||_{L^p(\Omega)}$, where Ω is a open connected locally compact Hausdorff space and use of $\overline{q}_{\Omega} = \frac{1}{|\Omega|}\int_{\Omega}\overline{q}\,(y)\,dy$ yields

$$\frac{\mathrm{d}E}{\mathrm{d}t} \leq -2\pi^2\,(1-n)\min\left\{1, \frac{a}{L_e\phi}\right\}E. \tag{35}$$

Equation (35) then guarantees that $E\,(t) \to 0$ as $t \to \infty$ for $0 < n < 1$. Applying the arithmetic-geometric mean inequality on Eq. (27) yields

$$||\overline{q}||^2 \leq ||\overline{\theta}||^2. \tag{36}$$

From Eqs. (36) and (29), it follows that the decay of $||\overline{q}||$ is implied by the decay of $E\,(t)$, and hence, the system is stable. From the above, we have identified that the nonlinear stability requires the critical argument at $n = 1$. The corresponding Euler–Lagrange system with the maximum problem Eq. (33) is

$$\xi\overline{\theta}\nabla\theta_s - \overline{\theta}\mathbf{k} + 2\overline{q} = \nabla\overline{\delta}, \tag{37}$$

$$\overline{w} - \xi\overline{q}\cdot\nabla\theta_s + 2\xi\nabla^2\overline{\theta} = 0. \tag{38}$$

Here $\overline{\delta}$ is a Lagrange multiplier introduced because $\overline{q}$ is divergence free. We consider R_z as the eigenvalue and estimate the maximum variation of R_z with optimal choice of ξ. Equations (37) and (38) yield

$$\frac{\partial R_z}{\partial\xi} = \frac{n\,(1-\xi R_z)\,||\nabla\overline{\theta}||^2 + \langle\widetilde{A}\overline{\theta}\overline{w}\rangle - R_x\langle\overline{\theta}\overline{u}\rangle + R_y\langle\overline{\theta}\overline{v}\rangle}{\xi^2\left(2n||\nabla\overline{\theta}||^2 + \langle\widetilde{A}\overline{\theta}\overline{w}\rangle - R_x\langle\overline{\theta}\overline{u}\rangle + R_y\langle\overline{\theta}\overline{v}\rangle\right)}. \tag{39}$$

Equation (39) is important and also noted that if $R_x = R_y = 0$ and $Q = 0$, we get

$$\frac{\partial R_z}{\partial\xi} = \frac{(1-\xi R_z)}{2\xi^2}. \tag{40}$$

Equation (40) is the same as the expressions reported by Guo and Kaloni [21]. We solve the system of Eqs. (37) and (38) in the presence of the critical value $n = 1$. To evaluate this system numerically, we apply $curlcurl$ of Eq. (37) and further use the third component of the resulting equation

$$\xi R_x\frac{\partial^2\overline{\theta}}{\partial x\partial z} + \xi R_y\frac{\partial^2\overline{\theta}}{\partial y\partial z} + \xi\nabla_1^2\left[\left(-R_z + \widetilde{A}\right)\overline{\theta}\right] + 2\nabla_1^2\overline{w} - \nabla_1^2\overline{\theta} - 2\left(\frac{\partial^2\overline{u}}{\partial x\partial z} + \frac{\partial^2\overline{v}}{\partial y\partial z}\right) = 0 \tag{41}$$

where $\nabla_1^2 = \left(\frac{\partial^2}{\partial x^2} + \frac{\partial^2}{\partial y^2}\right)$. Now, we apply the normal mode expansion

$$\left[\overline{q}, \overline{\theta}, \overline{\delta}\right] = [q\,(z)\,, \theta\,(z)\,, \delta\,(z)]\exp\left(i\,(kx + ly)\right), \tag{42}$$

with $\left(R_x, R_y\right)\cdot(k, l) = 0$, (Nield [26] and Kaloni and Qiao [22]), i.e., the horizontal thermal Rayleigh number vector is orthogonal to the wave number vector. We substitute (42) in Eqs. (37), (38) and (41) and eliminate u, v and δ to obtain

$$D^2w = \frac{\alpha^2}{2}\left(2w + \xi\left[-R_z + \widetilde{A}\right]\theta - \theta\right), \tag{43}$$

$$D^2\theta = \frac{1}{2}\left[-R_z + \widetilde{A} - \xi^{-1}\right]w + \left[\alpha^2 - \xi\left(\frac{R_x^2 + R_y^2}{4}\right)\right]\theta. \tag{44}$$

The system of Eqs. (43) and (44) is evaluated with the boundary conditions $w = \theta = 0$ at $z = \pm\frac{1}{2}$. The critical vertical thermal Rayleigh number is obtained as $R_z = \max_{\xi}\min_{\alpha^2} R_z$.

7 Results and discussion

The onset of thermal convection in a fluid-saturated porous layer in the presence of mass flow and an internal heat source effect is analyzed using both linear and nonlinear stability theory. Both cases are studied based on the classical normal mode technique. We treat the vertical thermal Rayleigh number as the eigenvalue R_z. Here, the critical vertical thermal Rayleigh number R_z is defined as the minimum of all R_z values as the wave number α is varied. The vector of wave number is defined as $\alpha = (k, l, 0)$. To achieve the stationary convection boundary, we set $\sigma = 0$ (the removal of the oscillatory mode is discussed in "Appendix"), with $\left(R_x, R_y\right) \cdot (k, l) = 0$. The longitudinal disturbances are characterized by $k = 0$. In the same way, transverse disturbances are characterized by $l = 0$. In Table 1, R_{z_l} and R_{z_e} indicate the linear and nonlinear critical thermal Rayleigh number (R_z). α_l and α_e indicate the critical wave number in linear and nonlinear cases.

From Table 1, it is observed that when $Q = 0$ and $M = 0$, in the linear case, the results are in very good agreement with earlier published results in the literature, Nield [26]. For an increase in the value of Q from 0 to 2, the critical value of R_z is reduced as seen in Table 1 in both cases. Hence, the heat flow parameter causes destabilization in the medium. A fixed notation is used to represent the curves corresponding to the linear and nonlinear results. Dotted lines represent linear stability results, and solid lines represent nonlinear stability results in Figs. 1, 2 and 3.

Table 1 Critical thermal Rayleigh numbers at $M = 0$

R_x	0	10	20	30	40
$Q = 0$					
R_{z_l}	39.4784	42.0076	49.5486	61.9566	78.9663
α_l	3.13999	3.1399	3.1499	3.1599	3.2199
R_{z_e}	39.47840	40.72345	44.20928	49.18550	53.61943
α_e	3.13999	3.08999	2.94999	2.7199	2.2799
$Q = 1$					
R_{z_l}	39.2360	41.7294	49.1460	61.2757	77.7028
α_l	3.1599	3.1599	3.1699	3.2099	3.3099
R_{z_e}	39.05626	40.27496	43.67935	48.51113	52.6681
α_e	3.15999	3.109999	2.96999	2.73999	2.28999
$Q = 2$					
R_{z_l}	38.53950	40.93195	47.99451	59.34272	74.11823
α_l	3.19999	3.19999	3.22999	3.33999	3.59999
R_{z_e}	37.85142	38.99556	42.16919	46.59001	49.8985
α_e	3.20999	3.15999	3.0299	2.7999	2.27999

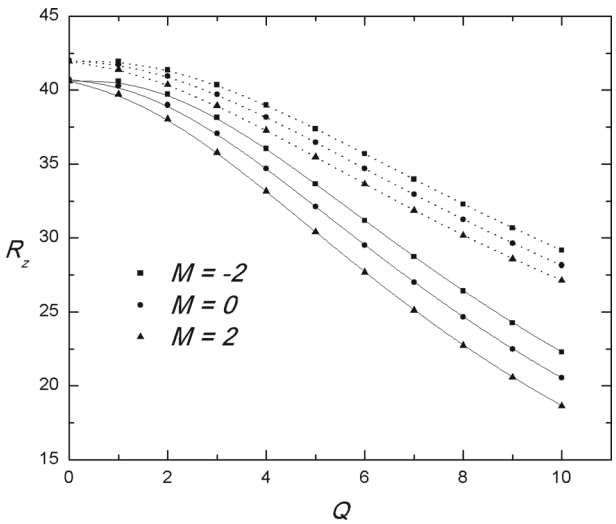

Fig. 1 Variation of R_z with Q at $R_x = 10$ and $R_y = 0$

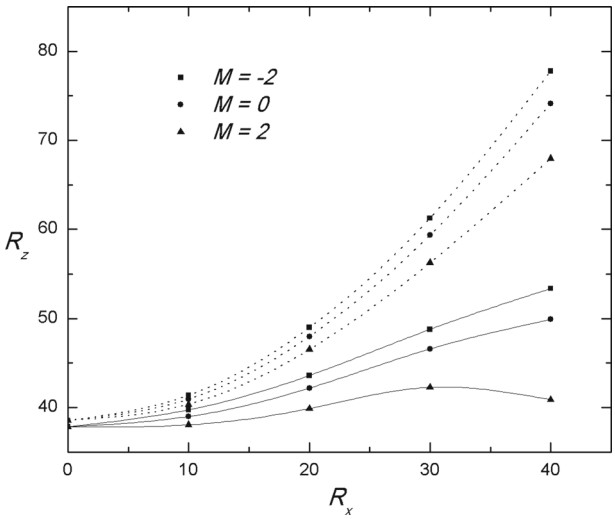

Fig. 2 Variation of R_z with R_x at $Q = 1$ and $R_y = 0$

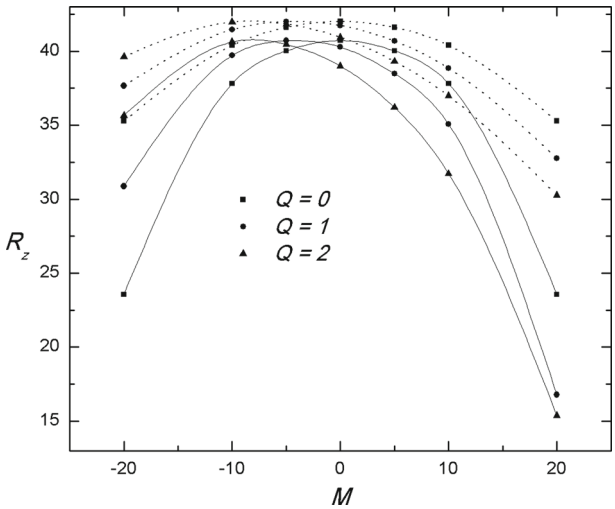

Fig. 3 Variation of R_z with M at $R_x = 10$ and $R_y = 0$

A comparison of the critical value of R_z as a function of Q for different values of the mass flow rate M is shown in Fig. 1 at $R_x = 10$ and $R_y = 0$. It is observed that as Q increases the critical values of R_z decrease. However, as M increases from -2 to 2, at a higher value of M, the critical R_z value is lower than at lower values of M in both the cases as seen in Fig. 1. For both positive and negative values of M, R_z decreases with increasing values of Q. It indicates that increasing the heat source has a strongly destabilizing effect. This is due to the fact that the global temperature of the system is increasing with increasing heat source and causes the instability. As increasing the heat source, the threshold critical region between linear and nonlinear results is increasing as seen in Fig. 1.

The response of R_z with varying R_x is shown in Fig. 2 for negative and positive values of M.

It is noted that, at $M = -2$ in the linear case, the critical value of R_z is higher than all the remaining values of M. When R_x is increased, the corresponding R_z values also increase for all M values. This indicates that the flow rate is strongly stabilizing in the linear case as compared to the nonlinear case seen in Fig. 2. It is also interesting to observe that as R_x increases the critical value of R_z also increases up to a certain value of R_x; thereafter, the R_z value decreases for $M = 2$ in the nonlinear case seen in Fig. 2. It means that the flow rate is strongly destabilizing at higher values of R_x and M in the nonlinear case.

Figure 3 shows the response of R_z with mass flow rate M in the presence of different values of $Q = 0, 1, 2$ for $R_x = 10$.

As the mass flow rate (M) increases, R_z also increases up to certain values of M and thereafter decreases for all values of Q as demonstrated in Fig. 3. Q has a strongly stabilizing effect up to a certain value of M, then after strongly destabilizing the flow in both cases. It is seen that by increasing the magnitude of horizontal mass flow in both negative and positive directions the critical value of $R_z$is decreased.

8 Conclusions

We have analyzed the instability of thermal convection in Hadley–Prats flow subject to an internal heat source using linear and nonlinear stability analysis. The results yield the following conclusions:

- An increase in the internal heat source causes a strong destabilization in all cases, as it raises the global temperature of the system.
- In the presence of horizontal mass flow, the flow is stabilizing at higher horizontal Rayleigh numbers in the linear case, whereas it is destabilizing in the nonlinear case at larger mass flows.
- Qualitative changes appear in R_z as the mass flow moves from negative to positive for different internal heat sources.

Acknowledgments The authors are grateful to the anonymous referees for remarks which improved the work considerably.

Appendix

In this section, we show that the imaginary part of σ is 0 (i.e., the oscillatory mode does not exist). After we use the condition $\left(R_x, R_y\right) \cdot (k, l) = 0$, Eqs. (25) and (26) are transformed as

$$\left(D^2 - \alpha^2\right) w + \alpha^2 \theta = 0, \tag{45}$$

$$\left(D^2 - \alpha^2 - \sigma - iMk\right) \theta - \left(D\widetilde{\theta}\right) w = 0, \tag{46}$$

subject to boundary conditions $w = \theta = 0$ at both the plates $z = \frac{1}{2}$ and $z = -\frac{1}{2}$. Eliminating θ, for a single equation obtained from Eqs. (45)–(46), yields

$$\left(D^2 - \alpha^2\right)^2 w - (\sigma + iMk)\left(D^2 - \alpha^2\right) w + \alpha^2 \left(D\widetilde{\theta}\right) w = 0. \tag{47}$$

Multiplying Eq. (47) by $\overline{w}$ (complex conjugate of w) and integrating by parts over $[-\frac{1}{2}, \frac{1}{2}]$, and using the boundary condition, we obtain

$$||D^2 w||^2 + 2\alpha^2 ||Dw||^2 + \alpha^4 ||w||^2 + (\sigma + iMk)\left(||Dw||^2 + \alpha^2 ||w||^2\right) + \alpha^2 \int_{-0.5}^{0.5} \left(D\widetilde{\theta}\right) |w|^2 \, \mathrm{d}z = 0. \tag{48}$$

Taking the imaginary part of Eq. (48) when $\sigma = \sigma_r + i\sigma_i$,

$$\sigma_i \left(||Dw||^2 + \alpha^2 ||w||^2\right) = -Mk \left(||Dw||^2 + \alpha^2 ||w||^2\right). \tag{49}$$

When $k = 0$, we have $\sigma_i \left(||Dw||^2 + \alpha^2 ||w||^2\right) = 0$, which implies $\sigma_i = 0$.
This shows that the stationary longitudinal mode is the only possible mode for the convection induced by horizontal mass flow as stated by Nield and Bejan [19] and Kaloni and Qiao [22].

References

1. Chen, X., Li, A.: An experimental study on particle deposition above near-wall heat source. Build. Environ. **81**, 139–149 (2014)
2. Aihara, T., Fu, W., Shimoyama, M.H.T.: Experimental study of heat and mass transfer from a horizontal cylinder in downward air–water mist flow with blockage effect. Exp. Therm. Fluid Sci. **3**, 623–631 (1990)
3. Bendrichi, G., Shemilt, L.W.: Mass transfer in horizontal flow channels with thermal gradients. Can. J. Chem. Eng. **75**, 1067–1074 (1997)

4. Kwon, O., Bae, K., Park, C.: Cooling characteristics of ground source heat pump with heat exchange methods. Renew. Energy **71**, 651–657 (2014)
5. Schwiderskei, W., Schwabh, J.A.: Convection experiments with electrolytically heated fluid layers. J. Fluid Mech. **48**, 703–719 (1971)
6. Trittond, J., Zarraua, M.N.: Convection in horizontal layers with internal heat generation. J. Fluid Mech. **30**, 21–31 (1967)
7. Roberts, P.H.: Convection in horizontal layers with internal heat generation: theory. J. Fluid Mech. **30**, 33–49 (1967)
8. Thirlby, R.: Convection in an internally heated layer. J. Fluid Mech. **44**, 673–693 (1970)
9. Parthiban, C., Patil, P.R.: Effect of non-uniform boundary temperatures on thermal instability in a porous medium with internal heat source. Int. Commun. Heat Mass Transf. **22**, 683–692 (1995)
10. Parthiban, C., Patil, P.R.: Thermal instability in an anisotropic porous medium with internal heat source and inclined temperature gradient. Int. Commun. Heat Mass Transf. **24**, 1049–1058 (1997)
11. Barletta, A., Celli, M., Nield, D.A.: Unstable buoyant flow in an inclined porous layer with an internal heat source. Int. J. Therm. Sci. **79**, 176–182 (2014)
12. Rionero, S., Straughan, B.: Convection in a porous medium with internal heat source and variable gravity effects. Int. J. Eng. Sci. **28**, 497–503 (1990)
13. Alex, S.M., Patil, P.R.: Effect of a variable gravity field on convection in an anisotropic porous medium with internal heat source and inclined temperature gradient. ASME J. Heat Transf. **124**, 144–150 (2002)
14. Hill, A.A.: Double-diffusive convection in a porous medium with a concentration based internal heat source. Proc. R. Soc. A **461**, 561–574 (2005)
15. Chamka, A.J., Raheem, A., Khaled, A.: Similarity solutions for hydromagnetic simultaneous heat and mass transfer by natural convection from an inclined plate with internal heat generation or absorption. J. Heat Mass Transf. **37**, 117–123 (2001)
16. Bhadauria, B.S.: Double diffusive convection in a saturated anisotropic porous layer with internal heat source. Transp. Porous Media **92**, 299–320 (2012)
17. Borujerdi, A., Noghrehabadi, A.R., Rees, D.A.S.: Onset of convection in a horizontal porous channel with uniform heat generation using a thermal nonequilibrium model. Transp. Porous Media **69**, 343–357 (2007)
18. Borujerdi, A.N., Noghrehabadi, A.R., Rees, D.A.S.: Influence of Darcy number on the onset of convection in a porous layer with a uniform heat source. Int. J. Therm. Sci. **47**, 1020–1025 (2008)
19. Nield, D.A., Bejan, A.: Convection in Porous Media. 4th edn. Springer, Berlin (2013)
20. Capone, F., Rionero, S.: Nonlinear stability of a convective motion in a porous layer driven by a horizontal temperature gradient, Continuum Mech. Thermodyn. **15**, 529–538 (2003)
21. Guo, J., Kaloni, P.N.: Nonlinear stability and convection induced by inclined thermal and solutal gradients. Z. Angew. Math. Phys. **46**, 645–654 (1995)
22. Kaloni, P.N., Qiao, Z.: Non-linear stability of convection in a porous medium with inclined temperature gradient. Int. J. Heat Mass Transf. **40**, 1611–1615 (1997)
23. Kaloni, P.N., Qiao, Z.: Nonlinear convection induced by inclined thermal and solutal gradients with mass flow. Contin. Mech. Thermodyn. **12**, 185–194 (2000)
24. Kaloni, P.N., Qiao, Z.: Non-linear convection in a porous medium with inclined temperature gradient and variable gravity effects. Int. J. Heat Mass Transf. **44**, 1585–1591 (2001)
25. Kaloni, P.M., Lou, J.X.: Nonlinear convection of a viscoelastic fluid with inclined temperature gradient. Contin. Mech. Thermodyn. **17**, 17–27 (2005)
26. Nield, D.A.: Convection in a porous medium with inclined temperature gradient: additional result. Int. J. Heat Mass Transf. **37**, 3021–3025 (1994)
27. Weber, J.E.: Convection in a porous medium with horizontal and vertical temperature gradients. Int. J. Heat Mass Transf. **17**, 241–248 (1974)
28. Nield, D.A.: Convection in a porous medium with inclined temperature gradient and horizontal mass flow. Heat Transf. **5**, 153–185 (1990)
29. Straughan, B.: The Energy Method, Stability, and Nonlinear Convection. Springer, New York (2010)